

INFLUENCE OF RETAINED AUSTENITE ON THE FRACTURE STRAIN AND TOUGHNESS IN TRIP-ASSISTED MULTIPHASE STEELS

G. Lacroix, Q. Furnémont, T. Pardoën and P. J. Jacques
Université catholique de Louvain, Département des Sciences des Matériaux et des Procédés,
IMAP, Place Sainte Barbe 2, B-1348, Louvain-la-Neuve, Belgium
e-mail : lacroix@imap.ucl.ac.be, pardoën@imap.ucl.ac.be, jacques@imap.ucl.ac.be

Abstract

TRIP-assisted multiphase steels exhibit excellent combinations of the properties required in forming operations. These properties result from a composite effect – the presence of hard phases (bainite, austenite, martensite) dispersed in a ductile matrix (ferrite) – and the strain-induced martensitic transformation (TRIP effect). However, in some circumstances, the appearance of the hard and brittle martensite drastically reduces the crack resistance and impairs some forming processes. The cracking initiation and tearing resistance of different steel grades has been measured in order to better understand the relationship between microstructure and fracture resistance. The influence of microstructural parameters are analysed by *in-situ* testing and characterised by SEM and OIM. The fracture toughness is shown to decrease significantly with increasing volume fraction of retained austenite.

1. Introduction

Over the last decades, numerous studies have shown that TRIP-assisted multiphase steels present improved properties of strength and uniform elongation. The TRIP effect acts like an additional dislocation source that brings about extra work-hardening [1]. Up to now, only plastic properties were characterised and modelled. However, hardly anything has been reported on the fracture resistance of these steels, even if this property is of primary importance for their future applications in the automotive industry.

TRIP-assisted multiphase steels initially contain 3 phases: ferrite, bainite and retained austenite. The austenite presents a particular composition that stabilizes it at room temperature and allows its transformation to martensite during plastic straining. This transformation and the apparition of a harder phase (martensite) lead to improved plastic properties. Two steps are necessary during the heat treatment in order to generate these typical microstructures: (i) an intercritical annealing for the formation of the ferritic matrix and the austenite, (ii) a partial bainite transformation for the austenite retention [2].

This study aims at characterising at the macro- and microscopic scales, the damaging process and fracture toughness of several TRIP-assisted multiphases steels and at understanding the link between the microstructure, the TRIP effect and the fracture properties.

2. Materials and Experimental Procedure

Three different steel grades were investigated differing essentially by the carbon content. Indeed, since an important parameter for the nucleation of damage sites is the presence of hard phases (like bainite, retained austenite and martensite), the proportion of these phases was changed by considering several carbon contents for the alloys. The chemical composition of these alloys is given in Table 1.

TABLE 1. Chemical composition of the investigated steels

wt. %	C	Si	Mn	P	S	Al	N
015C	0.15	1.5	1.5	0.012	0.02	0.04	0.007
03C	0.31	1.51	1.57	0.009	0.008	0.009	0.004
045C	0.46	1.49	1.54	0.008	0.006	0.05	0.006

After standard hot and cold rolling, several specimens were heat-treated following the thermal route described in the introduction in order to generate microstructures that exhibit the best combination of strength and uniform elongation during uniaxial tensile straining. Figs. 1 (a-c) correspond to SEM micrographs illustrating the microstructure of the three specimens. The second phases are always located around the ferrite grains and forms a continuous network in steels 03C and 045C. Table 2 presents the proportions of the different phases measured by X-ray diffraction and image analysis. It is worth nothing that the content of retained austenite increases with the carbon level.

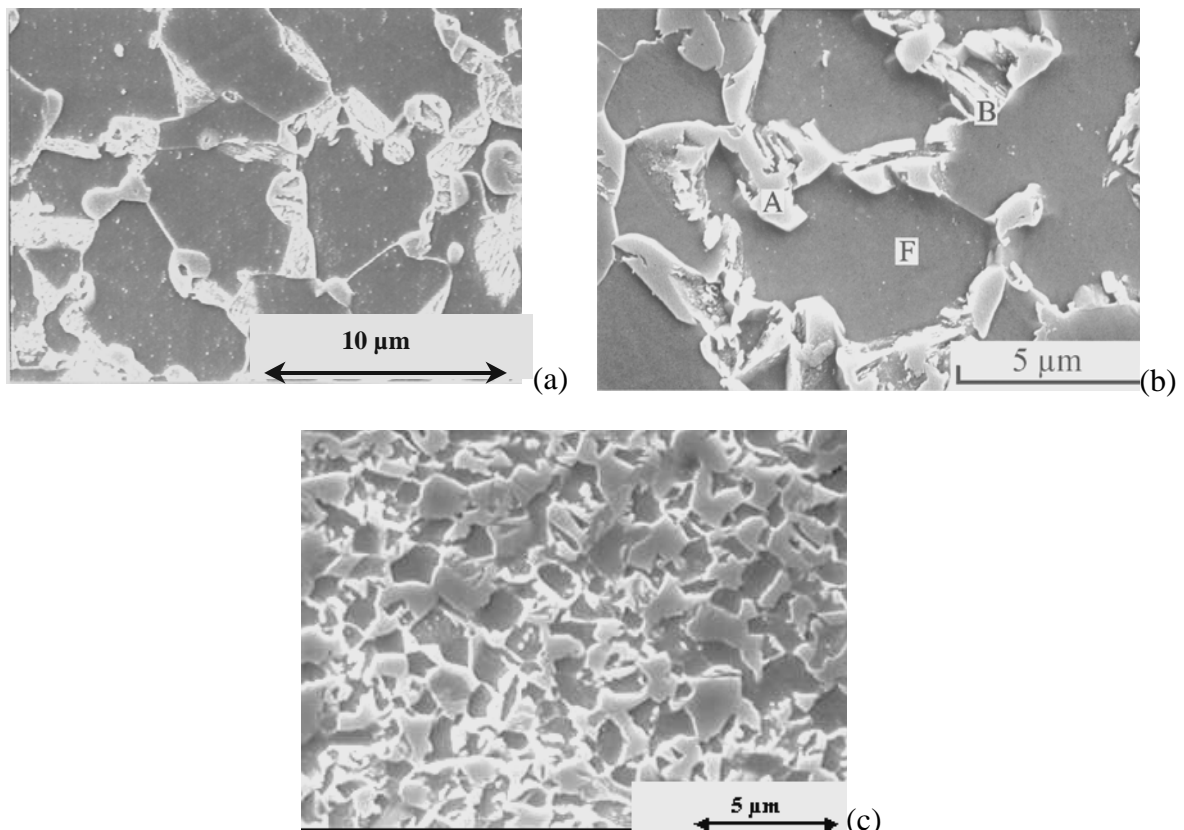


FIGURE 1: SEM micrographs of the microstructure of steels 015C (a), 03C (b) and 045C (c)

Table 2 : Proportion of the different phases present in the different steels

	Ferrite (α)	Bainite (α_b)	Austenite (γ)
015C	0.65	0.25	0.1
03C	0.55	0.27	0.18
045C	0.15	0.51	0.34

Fig. 2 presents the true stress – true strain curves for the three materials, respectively. This graph shows that the strength and work hardening increase with the proportion of second phase. However, steel 03C presents the best uniform elongation.

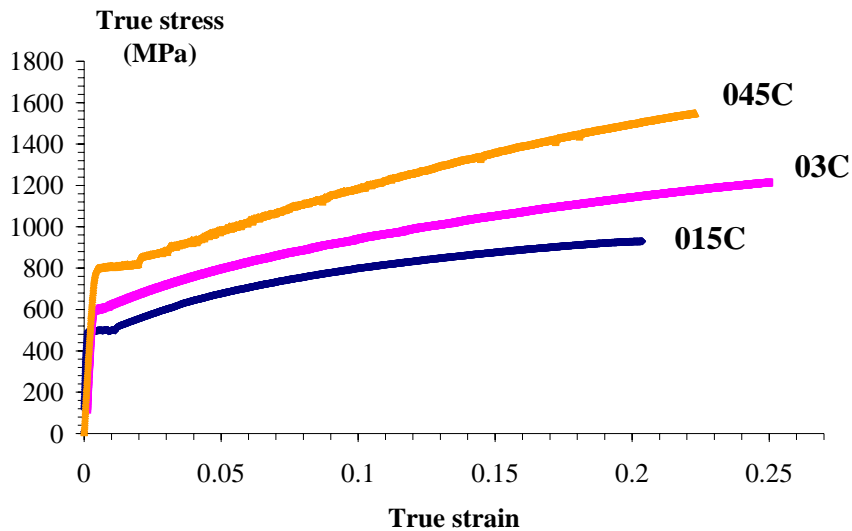


FIGURE 2: Uniaxial true stress - true strain of the 3 steel grades

Fracture toughness of the different steels was measured using the DENT geometry described in Fig. 3. The notches were first machined by EDM leading to a width of ~ 250 – 300 μm followed by a razor blade cutting. In order to satisfy the fracture mechanics assumption, fatigue precracking was also performed under the following conditions: $R=0.1$, $\Delta K= 0.2 \cdot K_{IC}$ (K_{IC} is the assumed toughness at initiation). The fatigue precracks were always longer than 300 μm .

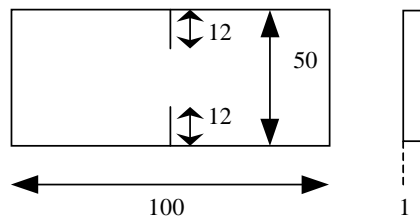


FIGURE 3: Geometry of the DENT samples (in mm)

The pre-cracked DENT specimens were loaded in tension. The test were interrupted after different amount of crack advance. Fig. 4 sketches the crack profile after some amounts of tearing and the measured parameters. In order to characterise the cracking resistance, the J integral and the crack advance Δa were determined for each specimen.

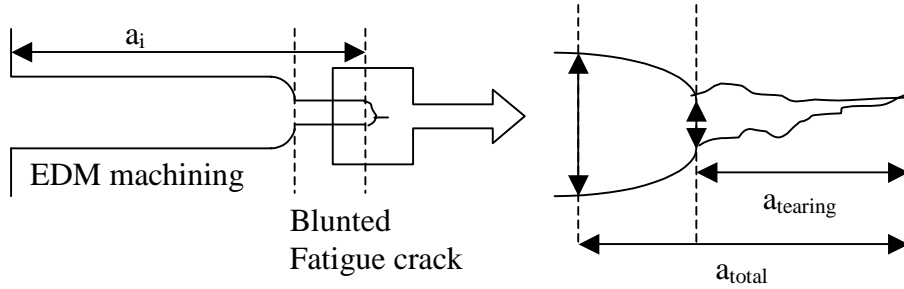


FIGURE 4: Schematic illustration of a crack tip

J was computed from the load-displacement curve as proposed by Rice *et al* [3]:

$$J_{Rice} = J_e + J_p = \frac{K_I^2}{E} + \frac{1}{l_0 t_0} \left(2 \int P du_p - P u_p \right) \quad (1)$$

where K_I is the stress intensity factor, E is the Young modulus, l_0 is the initial width between the two notches, t_0 is the thickness of the sample, P is the applied load and u_p is the plastic displacement.

The cracked specimens were also used for the characterisation of the damaging process. The specimens were first mechanically polished with diamond paste down to $1 \mu\text{m}$. The last step consisted in polishing with a silica colloidal suspension. Microstructure was characterised by orientation imaging microscopy (OIM). This technique allowed to quantify the proportion of transformed austenite around the crack tip. Furthermore, the microstructure was also revealed by nital (2%) etching and SEM observations in order to determine the crack path and the localisation of the damage sites.

3. Results and Discussion

The true fracture strain has been measured in order to better understand the mechanical behaviour of the different steels after necking. Indeed, this parameter can be related to the fracture resistance of the material. Fracture strain is evaluated from the measurement of the final fracture using cross-sectional area.

$$\varepsilon_{eq}^f = \sqrt{\frac{2}{9} \left[(\varepsilon_{11}^f - \varepsilon_{22}^f)^2 + (\varepsilon_{22}^f - \varepsilon_{33}^f)^2 + (\varepsilon_{33}^f - \varepsilon_{11}^f)^2 \right]} \quad (2)$$

where ε_{11}^f , ε_{22}^f and ε_{33}^f represent the fracture strain in the three principal directions. Table 3 gives the value of the different strain components and the corresponding equivalent strain at fracture.

Table 3: Fracture strains in the principal directions and the equivalent strain

	ϵ_{11}^f	ϵ_{22}^f	ϵ_{33}^f	ϵ_{eq}^f
015C	0.91	-0.05	-0.86	1.02
03C	0.52	-0.125	-0.39	0.54
045C	0.41	-0.11	-0.31	0.43

Table 3 indicates that the fracture strain decreases very rapidly with an increasing proportion of second phase. Furthermore, this decrease is more important between steels 015C and 03C.

The fracture toughness at crack initiation (J_{Ic}) extracted from the J_R curves are shown in Fig. 5, J_{Ic} decreases rapidly with the increase of the carbon level close in agreement with the fracture strains (see Table 3).

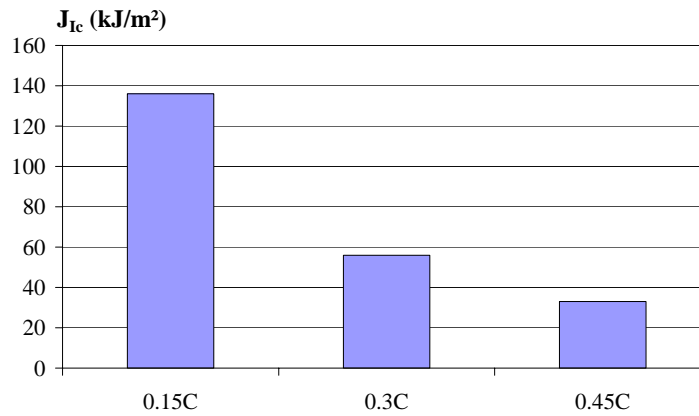


FIGURE 5: J_{Ic} for the 3 different specimens.

Fig. 6 presents the phase map measured by OIM at the tip of a crack in steel 045C. This map illustrates the influence of the stress field surrounding a crack on the TRIP effect. Indeed, a progressive transformation of the retained austenite (in white) into martensite (in black) can be observed depending on the distance from the crack tip. The fracture process zone (FPZ) size in this steel is typically equal to 10 μm . Indeed, the FPZ length is equal to about two times the critical CTOD (δ_c) which is roughly equal to $\alpha J_{Ic}/\sigma_0$, where α is the Shih factor in plane stress (here, $\alpha = 0.17$). It is clear that the stress triaxiality and the strain level at the crack tip are large enough to transform almost all the retained austenite inside the fracture process zone. The crack thus propagates in a microstructure containing large amounts of hard and brittle martensite (i.e. +/- 30%).

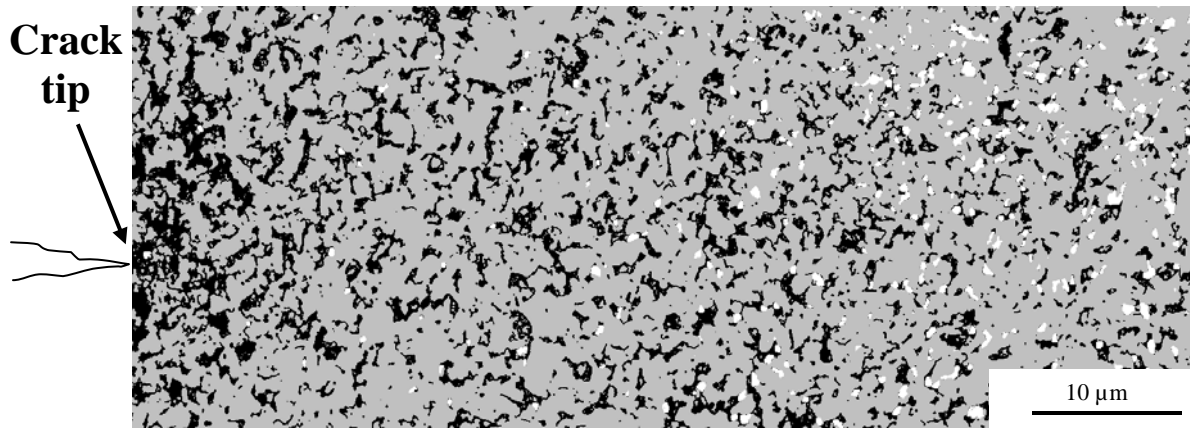


FIGURE 6: Phase map measured by OIM of a crack tip propagating in steel 045C (martensite in black, austenite in white, matrix of ferrite and bainite in grey)

Figs. 7 (a-d) present the microstructure around the crack tip in steel 03C. The micrographs were obtained by SEM after chemical etching. Figs. 7 (a) and (b) illustrate the crack path. The crack tends to follow the network of second phases that percolates throughout the microstructure along the grain boundaries of the ferrite phase. Figs. 7 (b), (c) and (d) emphasise the damage sites at different scales. They always consist in decohesion between martensite grains or between a ferrite grain and a martensite grain.

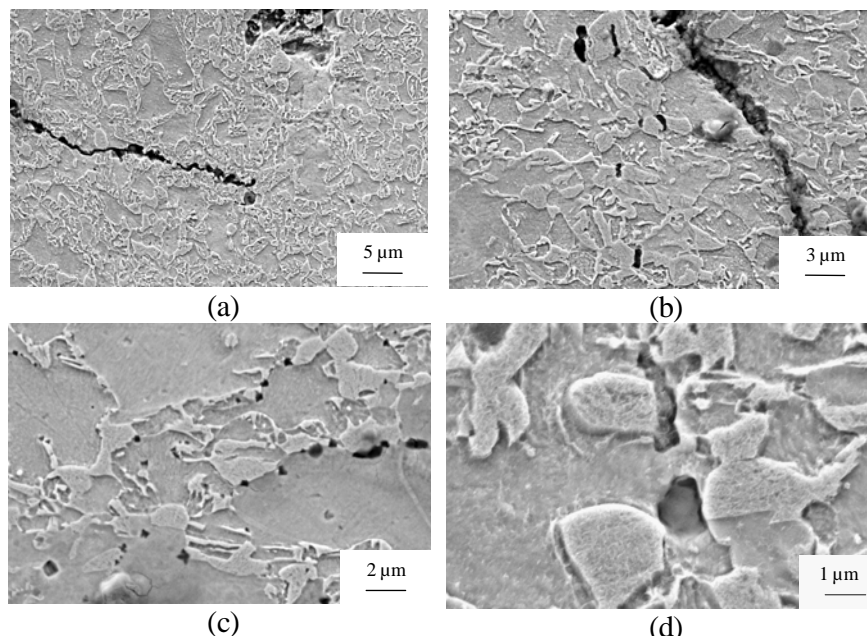


FIGURE 7: SEM micrographs illustrating the crack path and damage sites in steel 03C.

Figs. 6 and 7 showed that crack propagation occurs in a microstructure containing only martensite. This martensite plays a key role in the damaging process. If the carbon content increases, the austenite proportion also increases and consequently, more damage sites are present leading to smaller fracture toughness. Based on these observations, it can be assumed that all the voids nucleate by decohesion between the ductile ferritic matrix and the hard martensite [4].

With this assumption, fracture strain obtained experimentally can be roughly explained by applying a micromechanical model for void growth and coalescence in elastoplastic materials. This model is an extension of the Gurson analysis that accounts for initial void shapes that are not initially spherical [5]. The model considers an elastoplastic matrix characterised by isotropic elasticity with Young's modulus E and Poisson ratio ν , and by the J_2 flow theory. The uniaxial plastic flow behaviour is represented by $\sigma = \sigma_0(1 + k\varepsilon_{pl})^n$, where σ_0 is the yield strength and n is the strain hardening. The material contains an initial volume fraction f_0 of spherical voids with an aspect ratio W_0 . The effective strain is given by

$$\varepsilon_{ef} = F\left(\frac{\sigma_0}{E}, n, \nu, f_0, W_0\right) \quad (3).$$

Furthermore, f_0 can be estimated by

$$f_0 = \alpha W_0 f_p \quad (4)$$

where f_p is the proportion of second phase that initiates the voids, W_0 is the shape factor of the voids, and α represents the proportion of particles that gives rise to a void [6].

Applying this model to the 3 initial TRIP steels brings about the following interpretation for the different parameters:

- f_p : the second phase particules that initiate the voids are the transformed austenite grain (*i.e.* martensite). It is expected that all the austenite is transformed before necking so that f_p is equal to the proportion of austenite. The corresponding void nucleation kinetics is not taken into account here. This approximation is valid because the void growth rate is very small before necking.

- α : as shown on Fig. 7c, the number of voids and martensite grains are almost identical. α is thus supposed to be equal to 1.

- W_0 represents the initial aspect ratio of the voids which, when nucleating, are very small. It can be shown that if W_0 is taken sufficiently small, say $W_0 < 0.03$, the use of Eq. (4) to identify f_0 leads to fracture strains independents of W_0 [réf]. The W_0 is thus chosen equal to 0.01.

In summary, this model considers one fracture mechanism based on growth and coalescence of voids. The input of this model is essentially the volume fraction of second phases and flow properties. The difference of fracture strain difference observed experimentally between the steel grades can also be calculated by the model.

The predicted difference of fracture strain between steel 03C and 045C is equal to 0.15. This difference is comparable to the experimental results of Table 3. It suggests that the better fracture strain of steel 03C can be mainly due to the decreasing proportion of austenite.

When comparing steels 015C and 03C, the calculated difference of fracture strain is 0.2 which is smaller than the experimental result (0.48). In this case, the model allows to explain only a part of the increase of fracture strain. The other influencing parameter is probably the phase connectivity. Indeed, in steel 015C, the percolation of the second phase is not complete. It is important to stress that the void growth model is used here only as a qualitative tool, showing mostly that another effect than the second phase volume fraction has to be invoked to understand the different ductility of 03C and 015C steels.

This analysis of the fracture strain can also be carried out for toughness. Toughness improvement between steel 03C and steel 045C can be associated with the decreased

proportion of retained austenite. On the other hand, difference between steel 015C and steel 03C results not only from the smaller proportion of martensite in steel 015C but also of the isolated nature of these brittle grains.

4. Conclusion

This study has been carried out on steel grades differing by the retained austenite proportion. The following conclusions can be highlighted:

-The triaxiality and strain level at the crack tip are sufficient to transform all the retained austenite. Full transformation occurs in a region encompassing the fracture process zone length.

-All the damage sites are related to the presence of martensite. They mostly nucleate by decohesion between ferrite and martensite. Decohesion between martensite grains can also be observed.

-The crack propagates through void by void coalescence mechanism.

-Fracture strain and toughness indicate the same trends: fracture is easier when the carbon level and so the second phase proportion increase. With the assumption 'one martensite grain is equal to one void', it is possible to explain the increase of fracture strain between steels 03C and 045C. It suggests that the poor fracture strain is related to the initial proportion of retained austenite. For the difference between steels 03C and 015C, complementary explanation can be related to the decrease of the second phase connectivity.

Acknowledgement

G. Lacroix acknowledges the financial support of the FSR (UCL). P.J. Jacques is indebted to the FNRS and FRFC. This work was partly supported by the Belgian science policy within the framework of the PAI P5/08 project.

References

1. Jacques, P. J., Furnémont, Q., Mertens, A. and Delannay, F., *Philosophical Magazine A*, vol. **81** (7), 1789-1812, 2001.
2. Jacques, P. J., *Thermodynamics, Microstructures and plasticity*, Kluwer Academic Publishers, Dordrecht, The Netherlands, 2002.
3. Rice, J. R., Paris, P. C. and Merkle, J. G., *Progress in flaw growth and fracture toughness testing*, ASTM STP 536, p. 231, 1973.
4. Jacques, P. J., Furnémont, Q., Pardoën, T. and Delannay, F., *Acta Materialia*, vol. **49**, 139-152, 2001.
5. Pardoën, T. and Hutchinson, J. W., *Journal of the Mechanics and Physics of Solids*, vol. **48**, 2467-2512, 2000
6. Huber, G., Pardoën, T. and Bréchet, Y., *submitted for publication*.